

Probabilistic Modeling of Forced Ignition of Alternative Jet Fuels

Yihao Tang^{a,*}, Malik Hassanaly^{a,1}, Venkat Raman^a, Brandon Sforzo^b, Jerry Seitzman^c

^a*University of Michigan, 500 S State St, Ann Arbor 48109, USA*

^b*Argonne National Laboratory, 9700 S Cass Ave, Lemont 60439, USA*

^c*Georgia Institute of Technology, North Ave NW, Atlanta 30332, USA*

Abstract

Fast and reliable high altitude re-ignition is a critical requirement for the development of alternative jet fuels (AJFs). To achieve stable combustion, a spark kernel needs to transit in a partially or fully extinguished flow to develop a flame front. Understanding the relight characteristics of the AJFs is complicated by the chaoticity of the turbulent flow and variations in the spark properties. The focus of this study is the prediction of such characteristics by high-fidelity simulations, with a specific focus on fuel composition effect on the ignition process. For this purpose, a previously developed computational framework is applied, which utilizes high-fidelity LES simulations, a hybrid tabulation approach for modeling forced ignition and detailed quantification of uncertainty resulting from initial and boundary conditions to predict ignition probability. The method is applied to two alternative fuels (named C1 and C5) and Jet-A fuel (named A2) under gaseous conditions. Results show that the mixing of kernel and fuel-air mixture is not affected by the ignition process, but chemistry effects strongly dominate ignition probability. In particular, C1 exhibits much lower ignition probability than the other two fuels, especially at lean operating conditions. More importantly, this behavior is contradictory to ignition delay experiments which predict longer delay times for C5 compared to C1. Comparisons with experiments show that the comprehensive modeling approach captures the ignition trends. Analysis of kernel trajectories in composition space shows that the variations are caused by the relative effects of kernel mixing, response to strain, and ignition properties of the fuel.

Keywords: Forced ignition, High-altitude relight, Alternative jet fuels, Uncertainty quantification

*Corresponding author:

Email address: yhtang@umich.edu (Yihao Tang)

¹Currently at National Renewable Energy Laboratory (NREL)

1. Introduction

Alternative jet fuels (AJFs), from a variety of feedstocks and processes, are being considered as drop-in replacements for existing and future aircraft, with minimal to no modification of their operations [1]. An important requirement for commercial use is the ability to reliably and economically certify such fuels. One figure of merit (FOM) for such certification is altitude relight [2], where a combustor at high altitude is stabilized using a re-ignition procedure. In this regard, understanding the relative role of fuel properties on ignition behavior is important. From a testing and certification point of view, a robust procedure for computationally predicting ignition will provide a critical enabling tool [3]. The focus of this work is to demonstrate a comprehensive simulation procedure for estimating ignition probability for a range of fuels and to understand the impact of chemical properties on the ignition process.

Altitude relight is achieved using a spark source or plasma ignitor, which introduces high enthalpy fluid, and possibly ionized or free radical species into the combustor. Due to the relatively cold conditions, a highly viscous liquid injection will lead to poorly atomized droplet distribution, which will further complicate the ignition process [4]. The focus here is on the gas-phase mixing and chemical reactions that lead to the formation of a stabilized flame. In general, the injected kernel will undergo mixing with air and fuel, which will reduce its temperature. Hence, ignition and flame stabilization are highly sensitive to the local strain, mixing rates, and fuel ignition properties [5, 6]. In particular, variations in the turbulent flow field, as well as spark energy changes will have a first-order impact on the success or failure of the ignition process. Since turbulence is chaotic, and its state is represented only by a high-dimensional dynamical system [7, 8], precisely computing or measuring ignition is infeasible. As a result, even in well-controlled experiments, ignition can only be described probabilistically [9]. Hence, the main goal of modeling and experimental validation is to obtain the ignition probability for a set of operating conditions.

Modeling relight phenomenon requires two different sets of models and tools: a) detailed modeling of the complex interaction between the ignition source, fuel thermochemical properties, and the background turbulent flow; b) modeling the impact of stochastic parameters arising from the chaotic turbulent flow state and spark ignition variations. Many previous studies have addressed these challenges separately. To achieve high-fidelity prediction of the forced ignition process,

one strategy is to apply imposed initial conditions (e.g. chemical equilibrium or burnt composition) to either detailed/reduced kinetic [10] or existing reduced-order combustion models [11, 12]. In this approach, a small flame front is assumed to exist, which is then allowed to grow and stabilize. However, at conditions relevant to relight, the initial kernel development might occur at conditions that have very high strain rates that might extinguish a diffusion-limited flame kernel. In this regard, modeling energy deposition (ED) itself provides an additional physical handle on the process. However, the application of ED is often limited to full-chemistry based simulations [13, 14] as existing turbulent combustion models, such as flamelet-based approaches, rarely include the underlying physics of forced ignition. To quantify ignition probability, previous models mainly use non-reacting flow statistics and presumed semi-empirical relations between reaction and cold flow dynamics [15, 16].

Recently, a comprehensive modeling procedure that includes detailed modeling of ignition, as well as the uncertainties of the flow field, was developed by Tang et al. [17, 18]. This approach uses a hybrid tabulation method that takes into account the mixing-limited kernel growth followed by the diffusion-reaction balance of the flame development. The tabulation method was combined with LES to form a forward model for predicting ignition outcome. This approach was then combined with a polynomial chaos expansion based uncertainty quantification approach (PCE-UQ) to estimate the probability of ignition by treating the turbulent flow and spark characteristics as uncertain. Similar to the work of Triantafyllidis et al. [19], it was determined that for methane-air systems, the spark energy plays a critical role, but the turbulent flow can enable weaker spark kernels to survive and lead to successful ignition.

For AJFs, the problem is complicated by the variability in fuel composition. For instance, the H/C ratio of test fuels can be in the range of 1.9–2.2 but with ignition delay times that vary by a factor of 2 [2]. Full-scale combustor tests and rig tests showed that while there is a correlation with ignition delay measurements [20–22], the behavior is highly dependent on the global equivalence ratio as well as other operating conditions. However, there has been tremendous progress in the construction of chemical kinetic mechanisms for these fuels [23–25], which provides a baseline for high-fidelity computational modeling of the ignition process.

With this background, the focus of this work is to use the detailed ignition modeling procedure of Tang et al. [18] to predict ignition probability for different fu-

els. The focus is on gas-phase ignition to remove the effect of droplet evaporation on the process. The conventional Jet-A fuel (A2) along with two AJFs (C1 and C5, described below) that were studied in the National Jet Fuel Combustion Program [2] are investigated. Each fuel has a slightly different composition that alters its thermochemical properties. The experimental configuration corresponding to the stratified jet flow facility [26] is used. Details of the experimental configuration are provided in Sec. 2. The computational framework and simulation setup is explained in Sec. 3. Results of the study are presented in Sec. 4 including comparisons with experimental data.

2. Experimental configuration

The experimental configuration consists of a rectangular domain with a sunken igniter at the bottom [27]. Figure 1 provides a side view at its mid-plane. For the cases studied here, the igniter protrudes about 3.18 mm into the flow. The flow is divided into two streams using a splitter plate upstream of the domain inlet (left of Fig. 1). The main flow consists of the fuel mixed with air at a prescribed equivalence ratio ϕ . The fuel injection is carried out sufficiently upstream of Fig. 1 such that some level of mixing has been achieved [17]. However, the mixture is not homogeneous and there exist spatial-temporal fluctuations of equivalence ratio in the domain of interest. In addition to the main flow, a kernel flow consisting of air issues below the splitter plate with the same bulk velocity as the main flow.

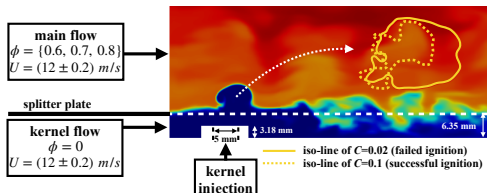


Figure 1: Schematic of the experimental setup. The cross-sectional area is 54 mm \times 85.7 mm. The contour is colored by equivalence ratio under a global value of 0.8.

In the following discussion, the term spark refers to the electric arc introduced during an igniter discharge, whereas a kernel is defined as the resulting high energy fluid pocket with no fuel present. An additional term flame kernel is defined as the fluid pocket with a high concentration of reaction products. After a spark discharge, the thermal expansion within the confined igniter cavity forces the kernel into the domain. The kernel needs to first transit through the non-flammable kernel flow before reaching the fuel-stratified reactive main flow. The ignition succeeds/fails depending on the competition between the kernel energy diffusion and the de-

velopment of an initial reaction towards a stable flame front. In this process, several factors play a role including the spark discharge, turbulence strain, fuel entrainment, and stratification. Multiple experimental studies [26, 27] have been performed using this facility for a range of operating conditions. More recently, numerical studies [14, 17, 18] have also been carried out, predominantly using methane-air mixtures.

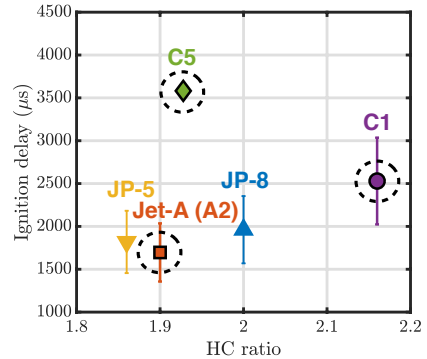


Figure 2: Diagram of the AJFs compared with conventional jet fuels. Fuels studied here are highlighted by circles. The ignition delay times [25, 28] are for fuel/air reactions at about 1000 K, 12 atm, and unity equivalence ratio. The C5 data is obtained from simulation.

The inflow temperature of the main flow and the kernel flow is set to 475 K. The fuels labeled C1, A2 and C5 in [2, 27] are tested, where A2 refers Jet-A fuel, while C1 and C5 are synthetic jet fuels designed for testing. C1 is composed of 99% iso-paraffins whereas C5 is composed of 73% iso-paraffins and 27% trimethylbenzene. Large variations of chemical properties can be found among the tested fuels, in particular, ignition characteristics as shown in Fig. 2. Based on available experiments, three global equivalence ratios of the main flow are considered ($\phi = \{0.6, 0.7, 0.8\}$) for each fuel leading to a total of 9 cases.

3. Computational framework

The comprehensive modeling framework is based on the procedure developed by the authors [18]. Figure 3 shows the simulation components. The main focus is on the hybrid tabulation and the sampling procedure, which together allow fuel variability effects to be included. Ignition predictions are conducted using the large eddy simulation (LES) approach. Only a brief description in the context of AJFs is provided here to motivate discussion. Readers are referred to [18] for details.

3.1. Hybrid tabulation for A2, C1, and C5 fuels

Tabulated chemistry is often used to include detailed chemical kinetics while reducing computational expense [29–31]. However, when multiple flame regimes

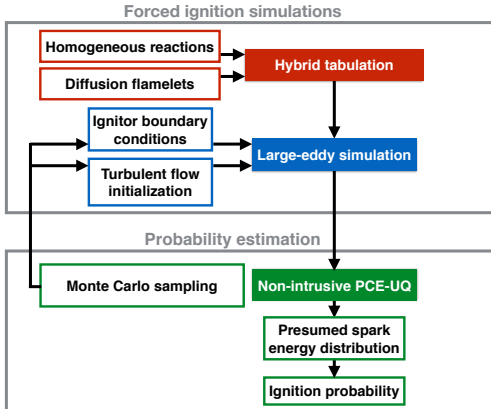


Figure 3: Diagram of the comprehensive computational framework for ignition probability prediction.

are present in a system, strategies for incorporating these regime changes are necessary [30]. In the hybrid method used here, two different canonical flows (homogeneous reactor HR, diffusion flamelet FPVA) are used to generate the lookup table as a function of progress variable (C), mixture fraction (Z) and enthalpy (H). The progress variable is defined as $C = Y_{H_2O} + Y_{CO_2} + Y_{CO} + Y_{H_2}$. In particular, the local total enthalpy, defined as the sum of sensible and formation enthalpies, is used to select the model regime, where the regime thresholds are obtained systematically [18]. The look-up table provides the source term of progress variable to the LES solver based on the local filtered mixture fraction, filtered progress variable, filtered enthalpy and filtered variance.

The HyChem family of chemistry mechanisms [24, 25, 28, 32] is used to perform the HR and FPVA calculations. Figure 4 shows the tabulated reaction source for the three fuels (see the caption for details). The spark kernel is initialized as energy deposition (ED) of high H with $C = 0$ that can propagate in a field of varying equivalence ratio or mixture fraction Z . The reaction rate obtained from HR calculations allows for the initiation of reactions even starting from a zero C . As the spark kernel moves through the flow field, entrainment of the cold fuel-air mixture reduces the total enthalpy, thereby transitioning to the FPVA region in the tabulation. It can be seen that there is a high reaction source $\omega_{C,A2}$ near $C = 0$ and a high H in Fig. 4, whereas classical FPVA tabulation, which only acts at low H , cannot ignite a mixture with zero progress variable. C1 can have either a largely higher or lower reaction source than A2 depending on the tabulation enthalpy, whereas C5 shows a consistently higher reaction source than A2. In this regard, C5 is more similar to A2 when compared to C1. This is mainly because C5 is chemically

more similar to A2 [2], whereas C1 produces a different combination of major pyrolysis from fuel decomposition [25]. The implications for the ignition probability of these different fuels are discussed in Sec. 4.

3.2. Kernel injection and uncertainty in boundary/initial conditions

To obtain ignition probability, the variability of the ignition process based on inflow and initial conditions is modeled. Here, the ignition kernel as well as the turbulent initial flow are considered uncertain. The kernel injection is modeled as a high-energy surface injection on the lower boundary, using a space-time-dependent Dirichlet boundary condition for the velocity and enthalpy fields. The enforced velocity profile is obtained by ensuring that the kernel trajectory matches experimental data. The enthalpy profile can be mapped from the energy deposited, as detailed in [18]. The total energy deposited is considered an uncertain parameter to model the shot-to-shot variability of the igniter. To model turbulence, the tabulation is incorporated into LES using a presumed-PDF approach [18]. A dynamic sub-grid-scale model [33] is applied to provide turbulent viscosity. An in house low-Mach solver [34] is used to perform this ensemble of LES. Prior to the main simulations, a cold flow LES is performed to construct a database of turbulent flow fields of $\{U, Z\}$, which is later applied to initialize the ignition simulations.

The ignition probability is estimated through a non-intrusive polynomial chaos expansion (PCE) [35] approach, where samples from the distribution of kernel energy and initial conditions are used to conduct multiple LES calculations. The ignition probability is estimated as the average outcome of these runs. Details of this procedure are explained in [18]. For these calculations, the shot-to-shot variability of the spark igniter needs to be prescribed. Since the igniter used here is the same as in [18], the spark characteristics are unchanged and prescribed as a normal distribution with a mean value of 1.24 J and standard deviation of 0.14 J. To achieve the same sampling accuracy as in [18], a total of 120 LES simulations were performed for each sampled case. The overall computational cost is about 1 million CPUh with a mesh with approximately 2 million control volumes.

4. Results

Figure 5 shows typical ignition success/failure time-sequences for each fuel considered, with identical kernel energy and operating conditions while randomly initialized turbulent states. Due to the pulsed-jet-in-

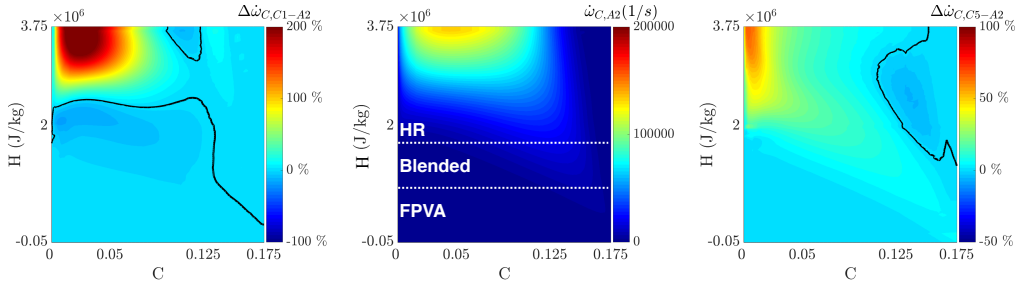


Figure 4: Contour of reaction source for A2 (middle) and the difference of C1 (left) and C5 (right) compared to A2 normalized as a percentage of $\dot{\omega}_{C,A2,max}$, plotted at equivalence ratio of 0.8. The black solid line marks the iso-value of zero difference between two compared tables.

crossflow type flow pattern, mixing is heavily dominated by the generation of counter-rotating vortex pairs. The time between $0.6 \sim 1.5$ ms is critical for ignition success, where a small reaction zone is generated through homogeneous ignition, leading to a ring-like OH-isosurface forming, with the high reaction progress variable concentrated at the bottom of the kernel and stabilizing on the lee-side of the jet. As time progresses, this high C region grows to encompass the entire OH isosurface. While the failed ignition cases show similar initial features (at 0.2 ms), the progress variable does not increase significantly beyond this time. The top view shows an asymmetry in the spanwise direction, which is realization dependent, with some cases showing stronger ignition fronts on the left lobe as opposed to the right lobe. Moreover, there are appreciable differences in the ignition structure for the three fuels. For instance, C1 shows a larger OH isosurface compared to C5 at 0.2 ms, but the kernel occupies a smaller volume at later stages. C1 also shows regions of high progress variable aligned with the core of the kernel, where the two counter-rotating pairs meet, compared to C5, which is similar in structure to A2. In the failed ignition case, C5 exhibits an appreciable reaction even at later times, but the kernel volume does not grow, indicating that the homogeneous reactions have not transitioned to a relatively low strain flame region. On the other hand, A2 and C1 fail similarly, with the progress variable dissipating due to entrainment of the colder fuel-air mixture.

To quantitatively evaluate model performance, the growth of the kernel area is compared with experimental data in Fig. 6. These simulations are conducted at a different operating condition of $\phi = 1.5$, since this is the only experimental data available. The kernel growth starts $1 - 2$ ms after kernel injection, which compared with Fig. 5 is when the transition from homogeneous reaction to flame kernel occurs. For all fuels considered, the model correctly predicts the ignition trends, with C1 showing the weakest growth rate. As pointed out ear-

lier, this arises from the slow oxidation of initial pyrolysis products [25]. C5 shows a slightly weaker growth rate in experiments and simulations compared to A2.

The ignition probabilities as a function of equivalence ratio along with the estimated uncertainty are shown in Fig. 7. For all three fuels, the ignition probability compares well with experimental data. Ignition probabilities over the range of lean equivalence ratios for each fuel generally increased with increased fuel content. Since C5 exhibits significant reactivity even for lower enthalpies, it is predicted to have the highest ignition probability among the three fuels considered here. Since C1 becomes less reactive at lower enthalpies compared to A2/C5, the kernel quenches more easily due to mixing. The plateau of ignition probability for C1 with increasing equivalence ratio is an illustration of the limit to the balance between the mixture reactivity and the cooling effect of that mixture as it is entrained into the kernel.

To understand the interaction between mixing and ignition, the kernel composition is probed using fluid particles. The particles are initialized within the kernel ($H \geq 2 \times 10^6$ J/kg) when its top edge reaches the main flow. For each LES simulation, a total of 1200 particles are tracked. The average of the particles trajectories is re-plotted in the phase space of interest, as shown in Fig. 8. In the left plot, the trajectories are interrogated in the 3D phase space of $H - \phi - C$. The projection onto the $H - \phi$ space is identical for all cases, indicating that mixing is nearly independent of the fuel. The differences between fuels are seen mainly in the variations of progress variable as a function of time. From the time histories of C and $\dot{\omega}_C$, a spike of $\dot{\omega}_C$ occurs about 0.2 ms, which leads to the first increment of C . The reaction is sharply suppressed after the initial spike, suggesting a fall-off of reaction rate due to the entrainment of colder flow. From Fig. 5, the time between $0.6 \sim 1.5$ ms is critical for ignition success, which corresponds to the time over which the reactions accelerate after the initial reduction. During this period, the C5 fuel exhibits the

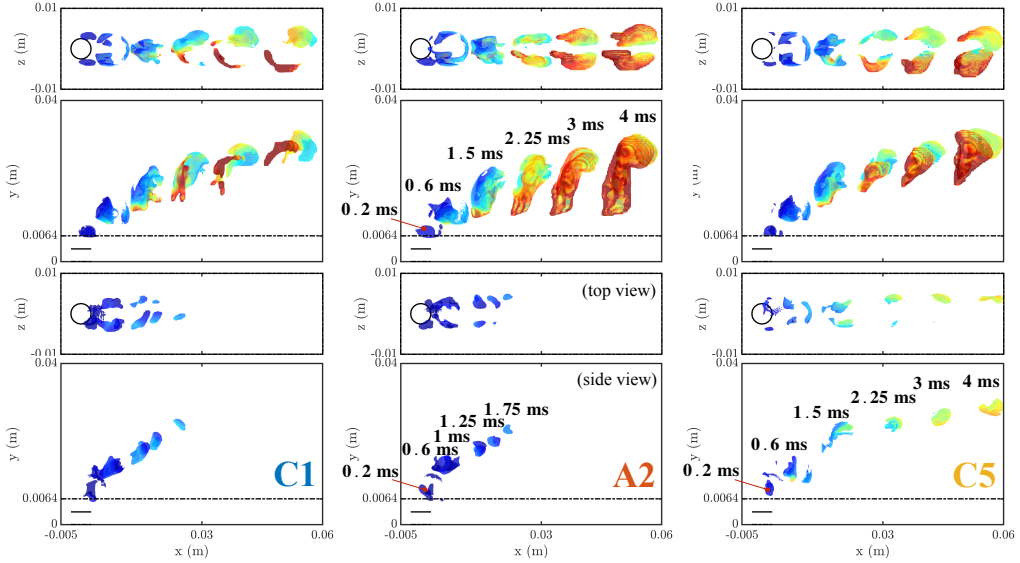


Figure 5: Isosurfaces of OH mass fraction $Y_{OH} = 5 \times 10^{-4}$ (top) and $Y_{OH} = 1 \times 10^{-4}$ (bottom) colored by progress variable $C \sim [0, 0.075]$ obtained from typical successful (top) / failed (bottom) ignition of C1 (left), A2 (middle) and C5 (right) fuel under $\phi = 0.8$. Dashed line indicates splitter plate height.

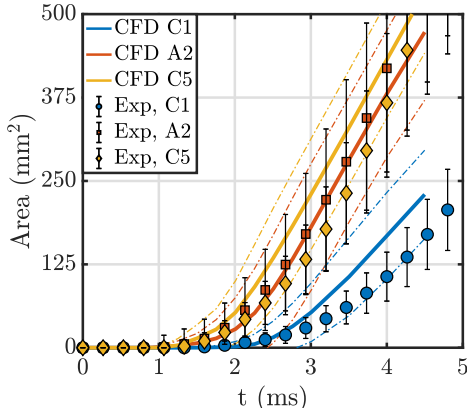


Figure 6: Kernel area growth history from 40 samples of successful ignition at $\phi = 1.5$. Experimental results [27] are obtained from chemiluminescence images. Numerical results are transformed from the flame kernel volume ($C \geq 0.275$) by assuming a spherical shape. Dash lines and error bars indicate a 95% confidence interval.

fastest restoration of $\dot{\omega}_C$, while the C1 fuel exhibits a restored value of $\dot{\omega}_C$ that is significantly lower than A2 and C5. After about 2 ms, the reaction rates reach a plateau, indicating the transition from homogeneous reaction to flame kernel. Figure 8 also shows the time histories of two of the major pyrolysis species. The main species is found to be C_2H_4 for A2 and C5, and i-C₄H₈ for C1. As i-C₄H₈ takes a much longer time than C_2H_4 to be oxidized [25], this chemical difference explains the overall weaker ignition strength of the C1 fuel, although pyrolysis products of C1 are generated at roughly the same rate as that for C5.

5. Conclusions

A comprehensive simulation approach was used to study forced ignition for three different fuels. The approach captures the experimental results and trends accurately for both flame kernel growth and ignition probability. Overall, C1 fuel exhibits a considerably weaker ignition process compared to A2 and C5. Fluid trajectory analysis reveals that the ignition process itself did not affect the fuel-air entrainment into the kernel. Hence, the observed differences come mainly from the interaction of the chemical processes with the particular trajectory in phase space introduced by the boundary and initial conditions. Specifically, the restoration of reaction rate from the initial reaction fall-off is critical for successful ignitions. In this regard, C1 exhibits a lower reaction rate than A2 and C5, possibly due to producing pyrolysis products that do not oxidize easily.

Acknowledgments

The authors gratefully acknowledge financial support from NASA through grant NNX16AP90A with Dr. Jeff Moder as the program monitor. The authors thank NASA HECC for the generous allocation of supercomputing time.

References

- [1] E. Corporan, T. Edwards, L. Shafer, M. J. DeWitt, C. Klingshirm, S. Zabarnick, Z. West, R. Striebich, J. Graham, J. Klein, Chemical, thermal stability, seal swell, and emissions studies of alternative jet fuels, *Energy & Fuels* 25 (3) (2011) 955–966.
- [2] M. Colket, J. Heyne, M. Rumizen, M. Gupta, T. Edwards, W. M.

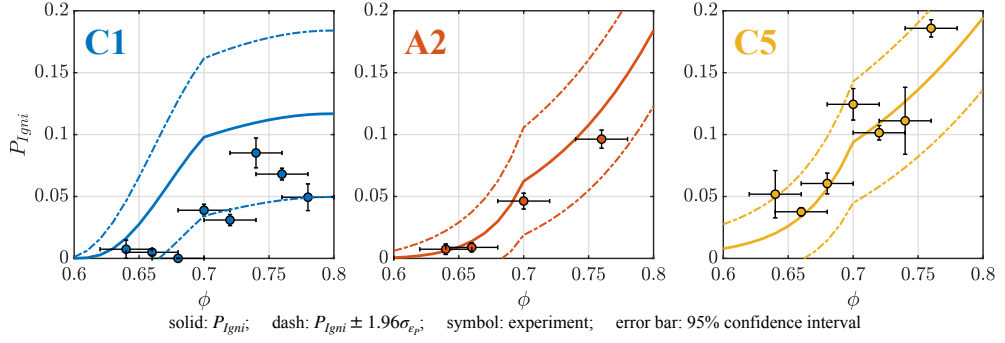


Figure 7: Comparison of numerical and experimental [27] ignition probability.

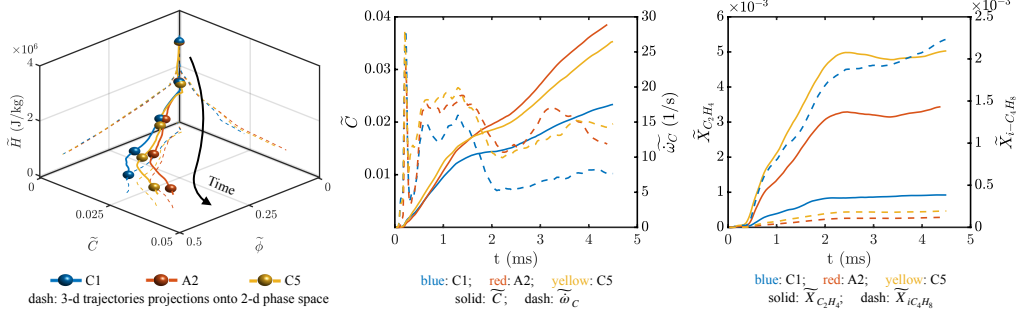


Figure 8: Ensemble-averaged fluid particle trajectories collected from successful ignition simulations at $\phi = 0.8$ and $E_d = 1.25 \text{ J}$.

- Roquemore, G. Andac, R. Boehm, J. Lovett, R. Williams, et al., Overview of the national jet fuels combustion program, AIAA Journal (2017) 1087–1104.
- [3] V. Raman, M. Hassanaly, Emerging trends in numerical simulations of combustion systems, Proceedings of the Combustion Institute 37 (2) (2019) 2073–2089.
 - [4] K. C. Opacich, J. S. Heyne, E. Peiffer, S. D. Stouffer, Analyzing the Relative Impact of Spray and Volatile Fuel Properties on Gas Turbine Combustor Ignition in Multiple Rig Geometries, AIAA Scitech 2019 Forum, AIAA 2019-1434, 2019, 2019.
 - [5] S. Ahmed, R. Balachandran, E. Mastorakos, Measurements of ignition probability in turbulent non-premixed counterflow flames, Proceedings of the Combustion Institute 31 (1) (2007) 1507–1513.
 - [6] A. Wawrzak, A. Tyliszczak, A spark ignition scenario in a temporally evolving mixing layer, Combustion and Flame 209 (2019) 353–356.
 - [7] P. Constantin, C. Foias, O. P. Manley, R. Temam, Determining modes and fractal dimension of turbulent flows, Journal of Fluid Mechanics 150 (1985) 427–440.
 - [8] M. Hassanaly, V. Raman, Ensemble-LES Analysis of Perturbation Response of Turbulent Partially-Premixed Flames, Proceedings of the Combustion Institute 37 (2019) 2249–2257.
 - [9] E. Mastorakos, Ignition of turbulent non-premixed flames, Progress in energy and combustion science 35 (1) (2009) 57–97.
 - [10] M. Boileau, G. Staffelbach, B. Cuenot, T. Poinsot, C. Bérat, Les of an ignition sequence in a gas turbine engine, Combustion and Flame 154 (1-2) (2008) 2–22.
 - [11] V. Subramanian, P. Domingo, L. Vervisch, Large eddy simulation of forced ignition of an annular bluff-body burner, Combustion and Flame 157 (3) (2010) 579–601.
 - [12] S. R. Stow, M. Zedda, A. Triantafyllidis, A. Garmory, E. Mastorakos, T. Mosbach, Conditional Moment Closure LES Modelling of an Aero-engine Combustor at Relight Conditions,

American Society of Mechanical Engineers, Paper GT2011-45100, 2011.

- [13] W. P. Jones, A. Tyliszczak, Large eddy simulation of spark ignition in a gas turbine combustor, Flow, turbulence and combustion 85 (3-4) (2010) 711–734.
- [14] T. Jaravel, J. Labahn, B. Sforzo, J. Seitzman, M. Ihme, Numerical study of the ignition behavior of a post-discharge kernel in a turbulent stratified crossflow, Proceedings of the Combustion Institute 37 (4) (2019) 5065–5072.
- [15] A. Neophytou, E. Richardson, E. Mastorakos, Spark ignition of turbulent recirculating non-premixed gas and spray flames: A model for predicting ignition probability, Combustion and Flame 159 (4) (2012) 1503–1522.
- [16] L. Esclapez, Numerical study of ignition and inter-sector flame propagation in gas turbine, Ph.D. thesis, Institut National Polytechnique de Toulouse (2015).
- [17] Y. Tang, M. Hassanaly, V. Raman, B. A. Sforzo, S. Wei, J. M. Seitzman, Simulation of gas turbine ignition using large eddy simulation approach, American Society of Mechanical Engineers, Paper GT2018-76216, 2018, 2018.
- [18] Y. Tang, M. Hassanaly, V. Raman, B. Sforzo, J. Seitzman, A comprehensive modeling procedure for estimating statistical properties of forced ignition, Combustion and Flame 206 (2019) 158–176.
- [19] A. Triantafyllidis, E. Mastorakos, R. Eggels, Large Eddy Simulations of forced ignition of a non-premixed bluff-body methane flame with Conditional Moment Closure, Combustion and Flame 156 (12) (2009) 2328–2345.
- [20] L. Rye, C. Wilson, The influence of alternative fuel composition on gas turbine ignition performance, Fuel 96 (2012) 277–283.
- [21] T. Mosbach, V. Burger, B. Gunasekaran, Fuel composition influence on gas turbine ignition and combustion performance, American Society of Mechanical Engineers, Paper GT2015-43020, 2015, 2015.
- [22] S. Blakey, L. Rye, C. W. Wilson, Aviation gas turbine alternative

- fuels: A review, *Proceedings of the combustion institute* 33 (2) (2011) 2863–2885.
- [23] S. Dooley, S. H. Won, F. M. Haas, J. S. Santner, Y. Ju, F. L. Dryer, T. Farouk, Development of reduced kinetic models for petroleum-derived and alternative jet fuels, 50th AIAA/ASME/SAE/ASEE Joint Propulsion Conference, AIAA 2014-3661, 2014.
 - [24] Y. Gao, T. Lu, Reduced HyChem models for jet fuel combustion, 10th US National Combustion Meeting, pp. 23-26, 2017.
 - [25] K. Wang, R. Xu, T. Parise, J. Shao, A. Movaghari, D. J. Lee, J.-W. Park, Y. Gao, T. Lu, F. N. Egolfopoulos, et al., A physics-based approach to modeling real-fuel combustion chemistry-IV. HyChem modeling of combustion kinetics of a bio-derived jet fuel and its blends with a conventional Jet A, *Combustion and Flame* 198 (2018) 477–489.
 - [26] B. A. Sforzo, High energy spark ignition in non-premixed flowing combustors, Ph.D. thesis, Georgia Institute of Technology (2014).
 - [27] B. Sforzo, H. Dao, S. Wei, J. Seitzman, Liquid fuel composition effects on forced, nonpremixed ignition, *Journal of Engineering for Gas Turbines and Power* 139 (3) (2017) 031509.
 - [28] R. Xu, K. Wang, S. Banerjee, J. Shao, T. Parise, Y. Zhu, S. Wang, A. Movaghari, D. J. Lee, R. Zhao, et al., A Physics-based approach to modeling real-fuel combustion chemistry-II. Reaction kinetic models of jet and rocket fuels, *Combustion and Flame* 193 (2018) 520–537.
 - [29] B. A. Perry, M. E. Mueller, A. R. Masri, A two mixture fraction flamelet model for large eddy simulation of turbulent flames with inhomogeneous inlets, *Proceedings of the Combustion Institute* 36 (2) (2017) 1767–1775.
 - [30] P.-D. Nguyen, L. Vervisch, V. Subramanian, P. Domingo, Multidimensional flamelet-generated manifolds for partially premixed combustion, *Combustion and Flame* 157 (1) (2010) 43–61.
 - [31] B. Fiorina, R. Vicquelin, P. Auzillon, N. Darabiha, O. Gicquel, D. Veynante, A filtered tabulated chemistry model for les of premixed combustion, *Combustion and Flame* 157 (3) (2010) 465–475.
 - [32] H. Wang, R. Xu, K. Wang, C. T. Bowman, R. K. Hanson, D. F. Davidson, K. Brezinsky, F. N. Egolfopoulos, A physics-based approach to modeling real-fuel combustion chemistry-i. evidence from experiments, and thermodynamic, chemical kinetic and statistical considerations, *Combustion and Flame* 193 (2018) 502–519.
 - [33] M. Germano, Turbulence: the filtering approach, *Journal of Fluid Mechanics* 238 (1992) 325–336.
 - [34] M. Hassanaly, H. Koo, C. F. Lietz, S. T. Chong, V. Raman, A minimally-dissipative low-Mach number solver for complex reacting flows in OpenFOAM, *Computer and Fluids* 162 (2018) 11–25.
 - [35] H. N. Najm, Uncertainty Quantification and Polynomial Chaos Techniques in Computational Fluid Dynamics, *Annual Review of Fluid Dynamics* 41 (2009) 35–52.